Technological Characteristics of Vanadyl Sulfate – Porous Silicon Heterojunction

Faiza M. Salim[1*]

Abstract

Near nano limit of [vanadium sulfate hydrate / porous silicon] heterojunction using zinc sulfide as a window for solar cell applications were investigated. Nanoparticles of vanadium sulfate hydrate were prepared by the electrochemical method followed by deposited in the form of thin films on bases of conductive glass and porous silicon to study the structural properties. The transmittance, absorbance and energy gap for the active material and the nanolayer window were performed. Grain size and roughness rate were determined via the surface topography test. The electrical parameters were measured, including the electrical conductivity. Nano crystalline porous silicon (PSi) films from p-type silicon (p - Si) wafer are synthesized using electrochemical etching (ECE) process of p-silicon wafer. Effective reflectance was obtained by ($ZnS/VOSO_4.H_2O/PSi/p$-Si) thin film that display excellent light-trapping at wavelengths ranging from (200 – 900) nm. The energy band gap of ($VOSO_4.H_2O$) NPs was calculated and found (4.2 - 5) eV. The average grain size ranged (67.7 – 82.9) nm. The electrical measurements current – voltage (I-V) were examined in dark and illumination conditions, for the heterojunctions fabricated. The efficiency of solar cell was reached (12.96%) while the power conversion efficiency was reached (51.8%).

Key Words: $VOSO_4.(H_2O)$, Nano-crystalline, Nanoparticles(NPs) Porous Silicon(PSi), Zinc Sulfide.

DOI Number: 10.14704/nq.2022.20.1.NQ22008 **NeuroQuantology 2022; 20(1):56-61**

Introduction

Nanomaterials are taking a big and fast evolution in recently since it has upright characteristics and possibility employments in a vast assortment of technological fields like photovoltaic applications (Paul, Bappi, *et al.* 2021). Porous Silicon (PSi)" which is made as a device bound the sir holes (pores) in silicon thin film" in nano size obtained strong luminescent properties, where it can be keened photoluminescence (PL) efficiency in the visible range of spectrum at room temperature (Martın-Palma, R.J., Pérez-Rigueiro, J. and Martınez-Duart, J.M., 1999). Sometimes, word nano porous used for a smallest - pore pattern to ensure the nanometric dimensions. The volumetric fraction of air of the material is called porosity (P %). the internal surface of PSi per unit volume can be very large, of the order of 500 m^2/cm^3 (Zilkie, A.J., Meier, J., Mojahedi, M., Poole, P.J., Barrios, P., Poitras, D., & Aitchison, J.S. 2007).

Vanadium (V^{23}) is a chemical element, it is a malleable transition metal exist naturally occurring element that is widely distributed in the environment in a number of minerals in oxidation states III, IV and V. In most of the minerals the vanadium is found as an oxide but occasionally it assumes the role of a metal cation. Vanadyl sulfate hydrate $VOSO_4.H_2O$, appears as a blue crystalline solid, denser than water and highly soluble in water. It is also generally stable under recommended storage conditions. Vanadyl sulfate is extremely toxic when ingested and great care should be taken not to touch or inhale the compound during use.

Corresponding author: Faiza M. Salim
Address: [1*]Department of Science, Opened Educational College, Ministry of Education, Iraq.
Relevant conflicts of interest/financial disclosures: The authors declare that the research was conducted in the absence of any commercial or financial relationships that could be construed as a potential conflict of interest.
Received: 04 November 2021 **Accepted:** 07 December 2021

Numerous literatures had been published on the subject of porous silicon and the use of the electrochemical etching method in addition to the method of preparing thin films using the droplet casting technique and studying the physical and technological properties of the membranes of the different systems for manufacturing solar cells with various windows of the type n or p like zinc sulfide, where these research provided important information in support of the research that followed; some of these literatures" ultraviolet to visible light sensing property of metal-semiconductor-metal was reported to enhance the optical properties of ZnS-PS: p-Si hybrid heterostructure (M Das, S Sarmah, D Sarkar 2021), the synthesis and the optical response of gold nanoparticles and thin nanostructured films grown by pulsed laser deposition are studied (M Ghidelli *et al.* 2018), the thermionic vacuum arc technology has found its firm place among the different procedures for thin film deposition (R Vladoiu *et al*. 2020)".

The Aims of the study summarized by preparation and characteristic of $VOSO_4.H_2O$ NPs prepared by using the hydrothermal method, and deposition on porous silicon and glass by the aid of drop casting method, then it will be studied its structural and morphological properties. As well as fabricated porous silicon substrate by the aid of electrochemical etching (ECE), and investigate its morphology and structural properties. Moreover, calculate the efficiency of (Ag / ZnS / $VOSO_4.H_2O$ / PSi / Si / Al) heterojunction as solar cell.

Theoretical Considerations

Solar cells are electrical devices with an optical and structural basis, through which light is invested to produce electrical energy. Therefore, it is very necessary to study the theoretical basis for the physical and technological characteristics for the components of the solar cell, since it is led to determine the efficiency of these cells. By studying X-ray diffraction (XRD), it is possible to determine the structural properties, including the rate of crystallite size (D). The rate of crystallite size can be calculated from the x-ray examination using the Sherrer formula (B Himabindu *et al.* 2021):

$$D = \frac{0{\cdot}94 \times \lambda}{\beta \times cos(\theta)} \qquad (1)$$

β: represent full width at half maximum (FWHM) measured by radian angles.

The dislocation density is the number of dislocations of lines that take off the unit area in that crystal. This is the percentage of total length of all dislocation lines, and crystal volume, in practices the density of the dislocations is measured using the giving relationship (C Shang *et al*. 2021):

$$\delta = \frac{1}{D^2} \qquad (2)$$

Where δ: is the dislocation density (Lines/(nm)^2), D: represent the average crystallite size (nm). Micro strain (ε) is a measure of the deformation of the material due to stress and tensile tension in the chain, which causes the lattice to continually deviate from its regular card value. The thin film's growth comes from the expansion of the compression within the crystalline lattice, which could be measured by the following equation (S Chattopadhyay *et al*. 2021):

$$\varepsilon = \frac{\beta \times cos\theta}{4} \qquad (3)$$

The optical properties of PSi have not been determined with enough resolution to confirm the quantum confinement model directly. The absorption edge of the band to band transition is affected by quantum confinement and it increases with the increase in the confinement energies of electrons and holes. It can be computed the energy gap according to the following equation [Y Matsuzaki *et al*. 2021]:

$$E_g\ (eV) = \frac{1240}{\lambda} \qquad (4)$$

Transmission represent the amount of intensity light rays (I) that penetrated the thin film produced, to the ratio of the fall light rays from the source (I_o) [Hegazy, H. *et al.* 2021]:

$$T = \frac{I}{I_0} \qquad (5)$$

Absorbance (A) defines by the ratio between the intensity radiations absorbed by thin films prepared (I_a) and the intensity incident radiation (I_o) (Goblet, M. *et al.* 2021):

$$A = \frac{I_a}{I_0} \qquad (6)$$

Absorption describes a reduction in electromagnetic radiation intensity when reaching a certain medium. Absorptions can be also being expressed in terms of transmission (T) and reflectivity (R) (Aggoune, W., *et al.* 2021):

$$A = 1 - T - R \qquad (7)$$

Reflectance (R) can be explained as the ratio of the reflected beam intensity (I_R) at the two-sided bordered and the intensity of the incident beam. Reflectivity is dependent upon the wavelength and nature of the surface of the thin film surface. It can be estimated based on the following relationship (Zhao, Y., *et al.* 2021):

$$R = \frac{I_0}{I_R} \qquad (8)$$

One of the most basic parameters of the electrical properties of a solar cell is the filling factor. It defines as the ratio between ability from heterojunction and real abilities (I_mV_m / I_{SC} V_{OC}). The ability can be obtained from the solar cell and can be written as the following relation (Green, M., *et al.* 2021):

$$F.F = \left[\frac{(I_mV_m)}{(I_{sc}V_{oc})}\right] \times 100\% \quad (9)$$

$$P_m = [I_mV_m] \quad (10)$$

Where V_m: highest voltage. I_m: highest current. P_m: maximum electrical power. Conversion efficiency (η) represents by the ratio between the biggest external electrical powers (P_m) to the incident light power (P_{in}) on an active area (A_{ac}), determine by relation (Akman, E., *et al.* 2021):

$$\eta = \left[\frac{(P_m)}{(P_{in}A_{ac})}\right] \times 100\% \quad (11)$$

The power conversion efficiency (*PCE*) is defined as "the percentage of the solar power that is changed from absorbed light to electrical energy" (Zhao, L., et al. 2021):

$$PCE = \left[\frac{(FF \times J_{sc} \times V_{oc})}{(P_{in})}\right] \times 100\% \quad (12)$$

Experimental

One of the most common way to prepare thin films solvent, which considered as the simplest method to fabricate thin films is (Drop casting method), where the nanoparticles prepared from ($VOSO_4.H_2O$) and mixed with distilled water. In addition to this composite process, the granulate material dissolved in the distilled water to prepare a solvent with heated the mixture then prepared specific concentration, at the last deposited on porous silicon and glass substrates.

Monocrystalline silicon wafer (p-type) having resistivity of (10 Ω.cm), and an orientation of (100). The porous of (p – type) silicon layers were fabricated by electrochemical etching where a p-type silicon substrate was placed in the Teflon etching cell using a mixture (1:1) of hydrofluoric acid (purity 40%) and ethanol (purity 99.99%) at room temperature. The substrates were cut into rectangles with areas of (1.5 × 1.5) cm^2. The sample was etched at a current density of (10) mA/cm^2 at etching time (10) min. After chemical treatment, (0.1) μm thick (Al) layers were deposited, by using an evaporation method, on the backsides of the silicon wafer as electric electrode, besides using (ZnS) to make window on the surface of ($VOSO_4.H_2O$) follow the making (Ag) electrode on the surface of (ZnS) layer.

In brief, the properties for this study included the structural, optical and electrical measurement for the active areas (A_{ac}) of (Ag / ZnS / $VOSO_4.H_2O$ / PSi / p-Si / Al) solar cell.

Result and Discussion

The results came in order to achieve the goals set for this study, which included the structural, optical and electrical properties of the heterojunction for the purpose of using there to improving the solar cell efficiency. The structural properties were verified through an x-ray examination. Figure (1) shows the XRD examination of the nanofilm ($VOSO_4.H_2O$) deposited on a glass base with one mole concentration. The result was matched with the standard card (this Figure shows peaks which agreement with the cards (JCPDS 20-1224: S, 73-0514: VO_2). The highest value of the compound was at the angle (2Θ = 13.09 ^{0}). From the matching it can be seen that the most of XRD peaks are indexed to hexagonal structure.

Figure (2), represents an X-ray test of each of the standard crystalline silicon thin film in addition to the porous silicon sample prepared as coming in the procedure of experimental work. A single strong, sharp and narrow peak is seen at 2θ = 69.14° oriented only along the (100) direction and confirming the single-crystal structure of the PSi layer, belonging to the reflective plane (100) of Si (According to ICDDN 1997 and 2011 JCPDS). Through the Figure, a wide sharp peak can be seen, and the slight width of the zigzag peaks can be explained as being due to the increase in the thickness of the porous silicon layer at the nano size. Through the XRD results, it was found that the porous silicon was formed into thin crystalline silicon, which helped to increase the absorption range of the visible spectrum.

Figure (3) summarizes the x-ray examination of the window material n - type (ZnS), and it can be seen from the Figure that the highest direction of growth of the compound was at the angle (2Θ = 27.9 ^{0}). All results of x – ray examinations are illustrated in Tables (1).

Table 1. XRD characteristics of PSi, ($VOSO_4.H_2O$) and ZnS.

Sample Type	2Θ deg.	β deg.	D nm	δ x 10^{-4} Lines / nm^2	ε x 10^{-4} (lines^{-2} nm^{-4})
PSi	69.14	2.28	60.79	2.70	82.16
$VOSO_4.H_2O$	13.09	0.236	33.47	8.92	8.44
ZnS	27.9	0.073	22.42	1.989	0.309

eISSN 1303-5150

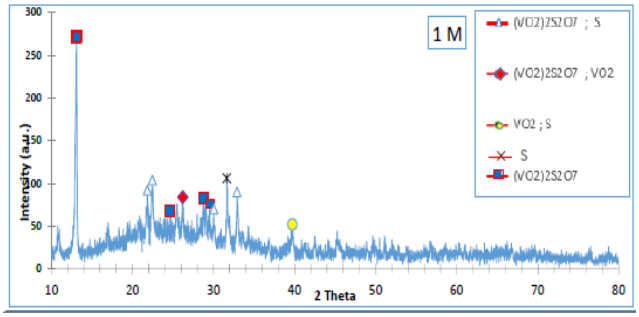

Figure 1. The XRD pattern of $VOSO_4.H_2O$ NPs solvent

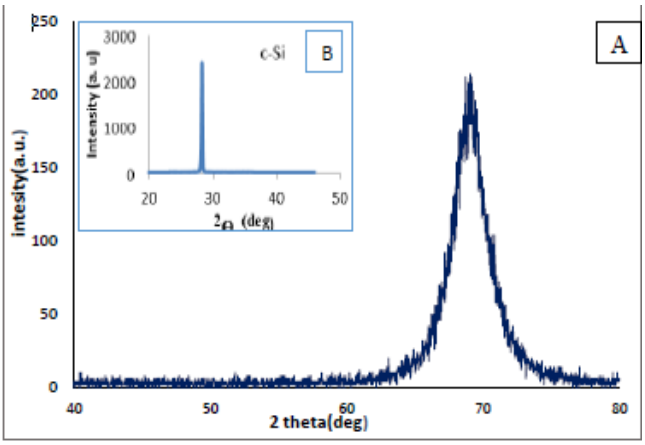

Figure 2. The XRD pattern: (A) of PSi sample anodized etching current density at (10) mA/cm^2 and etching time (10) min. (B) Crystalline Silicon wafer

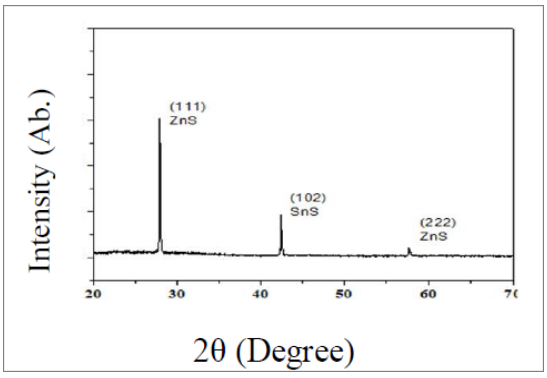

Figure 3. The XRD pattern of (n – ZnS) NPs

The specific investigation AFM images of PSi prepared from p-type silicon samples, which synthesis with fixed current density (10 mA/cm^2) and time etching (10 min) are illustrated the formation of uniform porous structure on the silicon wafer as shown in Figure (4). The pore average diameter, average roughness and root mean square have been estimated. Figure (4) shows 3D AFM image for PSi, $VOSO_4.H_2O$ and ZnS NPs. The morphology of the fabricated PSi layer by the AFM analyses is shown homogeneous and smooth structures. It has columnar grains measured from AFM analysis using software (imager 4.62) their average grain size, average roughness and the RMS are listed in Table (2). The AFM image of the irradiated surface exhibits coarser grind and rough surface.

Table 2. The Grain size, Roughness average and Root mean square of PSi. $VOSO_4.H_2O$ and ZnS.

Sample type	Grain size nm	Roughness nm	Root Mean Square nm
PSi	**82.9**	**18.9**	**9.7**
$VOSO_4.H_2O$	**45.92**	**2.34**	**2.7**
ZnS	**73.33**	**4.52**	**4.83**

Essential investigations on (PSi) show the result of an important signal of material represented via photoluminescence spectra of the (PSi / Si), ($VOSO_4.H_2O$ / PSi / Si) and (ZnS / $VOSO_4.H_2O$ / PSi / Si) heterojunctions as shown in Figure (5).

The emission peak of PSi are displayed at (770 nm) for the excitation wavelength at (650 nm). In this specific test, PL spectrum of NPs solution prepared with different concentration deposited on porous silicon (PSi) substrate, $VOSO_4.H_2O$/PSi heterojunction, the results done at room temperature with an excitation wavelength (550 nm), as illustrated in Figure (5). A single broad beak given at the area of green color 550 nm (2.25 eV) observed from the NPs fabricated films in (1 mole) concentration. The PL spectrum of (ZnS / $VOSO_4.H_2O$ / PSi / Si) shows the Gaussian curve.

Table (3) represents the measurement and calculations of electric properties to get the efficiency of the (Ag / ZnS / $VOSO_4.H_2O$ / PSi / Si / Al) heterojunction as the solar cells device.

Table 3. The parameters of I-V curve characteristics of active heterojunction solar cell

Sample type	*Voc* (V)	*Isc* [mA]	*Jsc* [mA /cm^2]	*Im* [mA]	*Vm* (V)	*F.F* %	*η* %	*PCE* %
Ag / PSi / Si / Al	**4.3**	**5.2**	**5.2**	**4.24**	**3.6**	**68.2**	**3.81**	**15.2**
Ag / $VOSO_4.H_2O$ /PSi / Si / Al	**7.25**	**8.8**	**8.8**	**6.76**	**4.9**	**51.9**	**8.28**	**33**
Ag / ZnS / $VOSO_4.H_2O$ /PSi / Si /Al	**6.92**	**12.8**	**12.8**	**9.6**	**5.4**	**58.5**	**12.96**	**51.8**

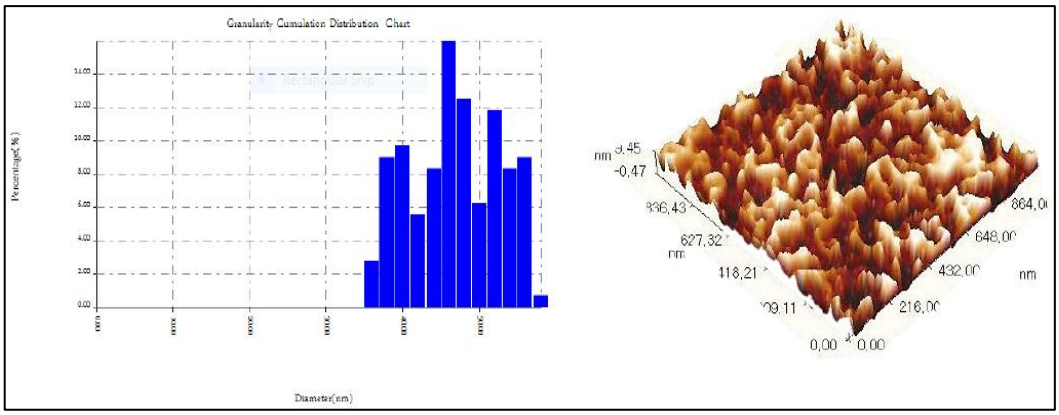

(a)

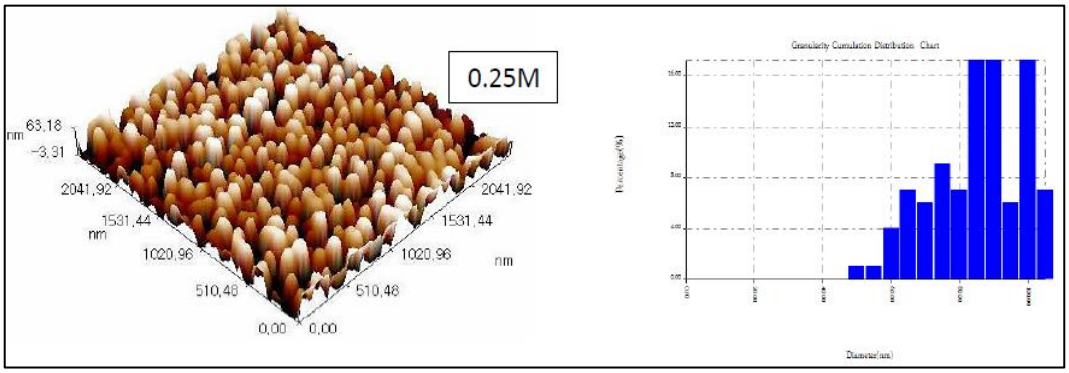

(b)

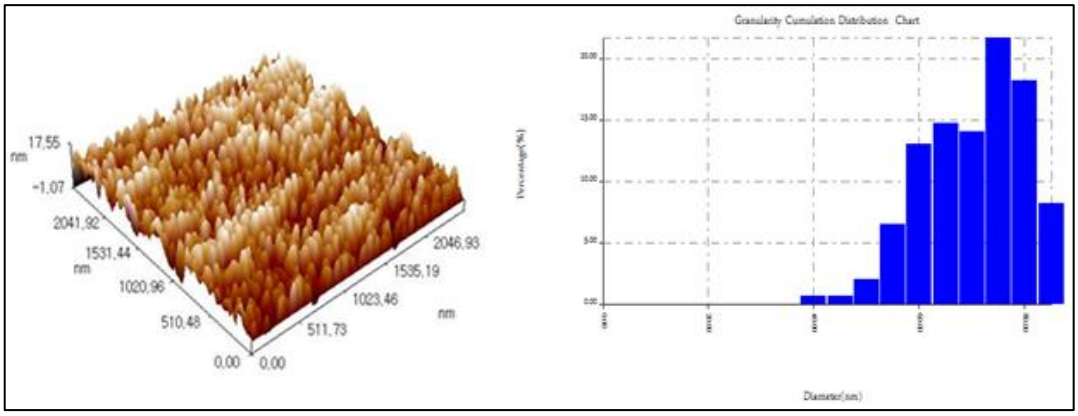

(c)

Figure 4. AFM of a) PSi, b) $VOSO_4.H_2O$ and c) ZnS NPs

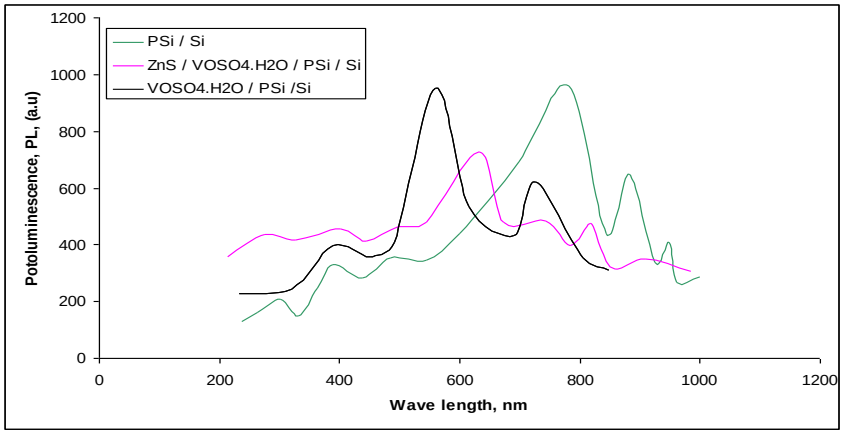

Figure 5. Photoluminescence spectra of the (PSi / Si), ($VOSO_4.H_2O$ / PSi / Si) and (ZnS / $VOSO_4.H_2O$ / PSi / Si) heterojunctions

*e*ISSN 1303-5150

Conclusions

Fabrication of heterojunction (Ag / ZnS / $VOSO_4.H_2O$ / PSi / p-Si / Al) by deposition of nanoparticles on the fabricated porous silicon and glass substrate, show good parameters and characteristic of the solar cell manufactured and enhanced the efficiency of the solar cell where the best efficiency observed for heterojunction (Ag / ZnS / $VOSO_4.H_2O$ / PSi / p-Si / Al) is 18.34 % by utilize the solvent concentration (1Mole).

References

Paul B, Bhanja P, Sharma S, Yamauchi Y, Alothman ZA, Wang ZL, Bhaumik, A. Morphologically controlled cobalt oxide nanoparticles for efficient oxygen evolution reaction. *Journal of Colloid and Interface Science*, 2021; 582: 322-332. https://doi.org/10.1016/j.jcis.2020.08.029

Martın-Palma RJ, Pérez-Rigueiro J, Martınez-Duart JM. Study of carrier transport in metal/porous silicon/Si structures. *Journal of Applied Physics* 1999; 86(12): 6911-6914. https://doi.org/10.1063/1.371772

Zilkie AJ, Meier J, Mojahedi M, Poole PJ, Barrios P, Poitras D, Aitchison JS. Carrier Dynamics of Quantum-Dot, Quantum-Dash, and Quantum-Well Semiconductor Optical Amplifiers Operating at 1.55$\mu {\hbox {m}} $. *IEEE Journal of Quantum Electronics* 2007; 43(11): 982-991. https://doi.org/10.1109/JQE.2007.904474

Das M, Sarmah S, Sarkar D. Distinct and enhanced ultraviolet to visible ZnS-porous silicon (PS): p-Si hybrid metal-semiconductor-metal (MSM) photodetector. *Materials Today: Proceedings*, 2021; 46: 6247-6252. https://doi.org/10.1016/j.matpr.2020.04.779

Ghidelli M, Mascaretti L, Bricchi BR, Zapelli A, Russo V, Casari CS, Bassi AL. Engineering plasmonic nanostructured surfaces by pulsed laser deposition. *Applied Surface Science* 2018; 434: 1064-1073. https://doi.org/10.1016/j.apsusc.2017.11.025

Vladoiu R, Tichý M, Mandes A, Dinca V, Kudrna P. Thermionic Vacuum Arc—A versatile technology for thin film deposition and its applications. *Coatings* 2020; 10(3). https://doi.org/10.3390/coatings10030211

Himabindu B, Devi NL, Kanth BR. (2021). Microstructural parameters from X-ray peak profile analysis by Williamson-Hall models; A review. *Materials Today: Proceedings*. https://doi.org/10.1016/j.matpr.2021.06.256

Shang C, Selvidge J, Hughes E, Norman JC, Taylor AA, Gossard AC, Bowers JE. A Pathway to Thin GaAs Virtual Substrate on On-Axis Si (001) with Ultralow Threading Dislocation Density. *Physica status solidi (a)* 2021; 218(3). https://doi.org/10.1002/pssa.202000402

Chattopadhyay S, Kumawat A, Misra KP, Halder N, Bandyopadhyay A, Antony A, Misra RDK. Micro-strain administered SHG intensity enhancement by heavy Ce doping in co-precipitated ZnO nanoparticles. *Materials Science and Engineering: B* 2021; 266. https://doi.org/10.1016/j.mseb.2021.115041

Matsuzaki Y, Hakoshima H, Sugisaki K, Seki Y, Kawabata S. Direct estimation of the energy gap between the ground state and excited state with quantum annealing. *Japanese Journal of Applied Physics* 2021; 60(SB). https://doi.org/10.35848/1347-4065/abdf20

Hegazy HH, Al-Buriahi MS, Alresheedi F, Alraddadi S, Arslan H, Algarni H. The effects of TeO_2 on polarizability, optical transmission, and photon/neutron attenuation properties of boro-zinc-tellurite glasses. *Journal of Inorganic and Organometallic Polymers and Materials* 2021; 31(6): 2331-2338. https://doi.org/10.1007/s10904-021-01933-2

Goblet M, Matin F, Lenarz T, Paasche G. Optical absorbance of the tympanic membrane in rat and human samples. *Plos one* 2021; 16(7). https://doi.org/10.1371/journal.pone.0254902.

Aggoune W, Irmscher K, Nabok D, Vona C, Anooz SB, Galazka Z, Draxl C. Fingerprints of optical absorption in the perovskite LaInO 3: Insight from many-body theory and experiment. *Physical Review B* 2021; 103(11). https://doi.org/10.1103/PhysRevB.103.115105.

Zhao Y, Zhu J, Wang H, Ma Z, Gao L, Liu Y, He J. Enhanced optical reflectivity and electrical properties in perovskite functional ceramics by inhibiting oxygen vacancy formation. *Ceramics International* 2021; 47(4): 5549-5558. https://doi.org/10.1016/j.ceramint.2020.10.139

Green M, Dunlop E, Hohl-Ebinger J, Yoshita M, Kopidakis N, Hao X. Solar cell efficiency tables (version 57). *Progress in photovoltaics: research and applications* 2021; 29(1): 3-15. http://doi.org/10.1002/pip.3371

Akman E, Shalan AE, Sadegh F, Akin S. Moisture-Resistant $FAPbI_3$ Perovskite Solar Cell with 22.25% Power Conversion Efficiency through Pentafluorobenzyl Phosphonic Acid Passivation. *ChemSusChem* 2021; 14(4): 1176-1183. https://doi.org/10.1002/cssc.202002707

Zhao L, Duan J, Liu L, Wang J, Duan Y, Vaillant-Roca L, Tang Q. Boosting power conversion efficiency by hybrid triboelectric nanogenerator/silicon tandem solar cell toward rain energy harvesting. *Nano Energy* 2021; 82. https://doi.org/10.1016/j.nanoen.2021.105773

Alshrefi SM, Al-Mamoori MHK, Jader MJ. Effect of 532 NM KTP ND: YAG laser on poly methyl methacrylate polymer optical properties. *NeuroQuantology* 2020; 18(2): 133-137.